

3-D compact explicit-finite difference time domain scheme for density variation

密度変化を組み込んだ3次元CE-FDTD法

Takao Tsuchiya^{1†} and Naoki Maruta¹ (¹Faculty of Science and Engineering, Doshisha Univ.)

土屋隆生^{1†}, 丸田直樹¹(¹同志社大・理工)

1. Introduction

The finite-difference time-domain (FDTD) method [1] is widely used to analyze the sound wave propagation. In some derivative methods of FDTD method, the compact explicit FDTD (CE-FDTD) method [2-4] recently attracts much attention because of its high-accuracy. It is a wave equation based scheme and a high-accuracy version of the standard FDTD method. However, it is difficult to analyze sound wave propagation in density varying media by the CE-FDTD method because the density does not appear in the wave equation explicitly. In this study, the density variation is implemented in the 3-D CE-FDTD method. Some demonstrations are carried out for the three dimensional sound wave propagation.

2. Theory

The 3-D wave equation on the sound pressure p is given as

$$\frac{1}{c_0^2} \frac{\partial^2 p}{\partial t^2} = \frac{\partial^2 p}{\partial x^2} + \frac{\partial^2 p}{\partial y^2} + \frac{\partial^2 p}{\partial z^2} \quad (1)$$

where c_0 is the sound speed. In the CE-FDTD method, the wave equation is directly discretized on the collocated grid on the basis of the central finite-difference method. There are 27 grid points or nodes in a discretized cell of the CE-FDTD method, as shown in Fig. 1. The grid intervals of x-, y-, and z-directions are assumed to be all the same, Δ .

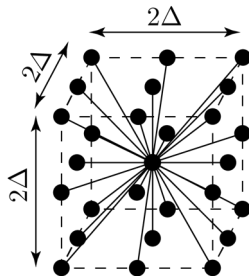


Fig. 1 Cell used in the CE-FDTD method consists of 27 grid points.

Considering not only the axis directions but also the face diagonal and the space diagonal directions, Eq. (1) is discretized as [2]

$$\delta_t^2 p_{i,j,k}^n = \chi^2 [(\delta_x^2 + \delta_y^2 + \delta_z^2) + a(\delta_x^2 \delta_y^2 + \delta_y^2 \delta_z^2 + \delta_z^2 \delta_x^2) + b\delta_x^2 \delta_y^2 \delta_z^2] p_{i,j,k}^n \quad (2)$$

where $p_{i,j,k}^n$ represents the sound pressure at the grid point $(x, y, z) = (i\Delta, j\Delta, k\Delta)$ at time $t = n\Delta t$, Δt is time step, $\chi = c_0 \Delta t / \Delta$ is the Courant number, a and b denote numerical parameters. δ^2 is an operator on the central finite difference. For example,

$$\delta_x^2 p_{i,j,k}^n = p_{i+1,j,k}^n - 2p_{i,j,k}^n + p_{i-1,j,k}^n \quad (3)$$

In the CE-FDTD method, there are some derivative schemes by adjusting the parameters a and b . In the case of $a = 0, b = 0$, the scheme is well known as the standard leapfrog (SLF) scheme. The most accurate scheme is the interpolated wideband (IWB) scheme ($a = 1/4, b = 1/16$) in which the cut-off frequency is in agreement with the Nyquist frequency.

For the density variation, it is necessary to begin the formulation from the continuity equation and the equation of motion, because the density is not appeared in the wave equation explicitly. In these governing equations, the particle velocity is defined on the center of the grid points, so the density ρ is evaluated as the average between the adjacent cells as shown in Fig. 2. Consequently, the central differences in Eq. (2) are rewritten as

$$\delta_x^2 p_{i,j,k}^n = 2\rho_{i,j,k} \left(\frac{p_{i+1,j,k}^n - p_{i,j,k}^n}{\rho_{i+1,j,k} - \rho_{i,j,k}} - \frac{p_{i,j,k}^n - p_{i-1,j,k}^n}{\rho_{i,j,k} - \rho_{i-1,j,k}} \right) \quad (4)$$

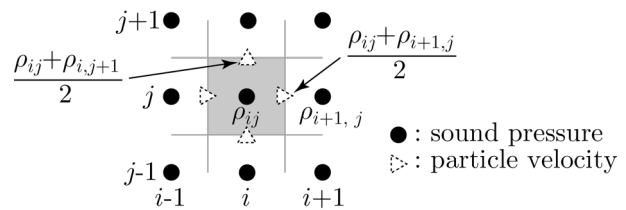


Fig. 2 Cells of CE-FDTD method and the definition of density (illustrated in 2-D).

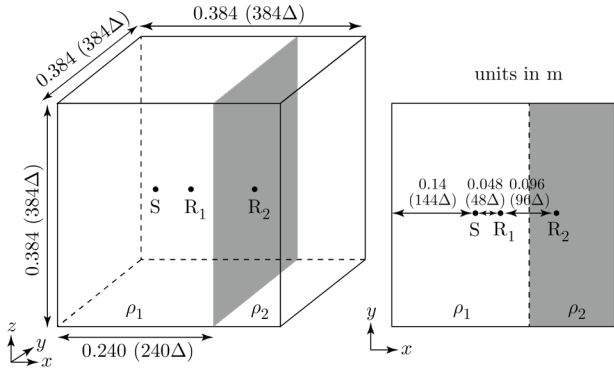


Fig. 3 Numerical model.

$$\delta_x^2 \delta_y^2 p_{i,j,k}^n = 2\rho_{i,j,k} \left(\frac{\delta_y^2 p_{i+1,j,k}^n - \delta_y^2 p_{i,j,k}^n - \delta_y^2 p_{i,j,k}^n + \delta_y^2 p_{i-1,j,k}^n}{\rho_{i+1,j,k} - \rho_{i,j,k}} \right) \quad (5)$$

$$\delta_x^2 \delta_y^2 \delta_z^2 p_{i,j,k}^n = 2\rho_{i,j,k} \left(\frac{\delta_y^2 \delta_z^2 p_{i+1,j,k}^n - \delta_y^2 \delta_z^2 p_{i,j,k}^n - \delta_y^2 \delta_z^2 p_{i,j,k}^n + \delta_y^2 \delta_z^2 p_{i-1,j,k}^n}{\rho_{i+1,j,k} - \rho_{i,j,k}} \right) \quad (6)$$

where $\rho_{i,j,k}$ denotes the density of cell on the grid point (i, j, k) .

3. Numerical experiments

Figure 3 shows a 3-D model for the density variation. The base medium is assumed to be water ($\rho_1 = 1000 \text{ kg/m}^3$, $c_1 = 1500 \text{ m/s}$), and another medium is $\rho_2 = 3000 \text{ kg/m}^3$, $c_1 = 1500 \text{ m/s}$. The grid size is $\Delta = 1 \text{ mm}$, the time step is $\Delta t = 0.667 \mu\text{s}$, so the Courant number is $\chi = 1$. A Gaussian pulse with width of $33.3 \mu\text{s}$ is radiated from the point source S, and received at R1 and R2. Figure 4 shows the sound pressure distributions when $t=40, 80, 120,$ and $160 \mu\text{s}$. There is a reflection observed at the interface between two media.

Figure 5 shows the calculated sound pressure waveforms at the receiving points R1 and R2. It is confirmed the reflected and transmitted waves. The reflection coefficient and the transmission coefficients are then estimated from calculated waveforms. Figure 6 shows the numerical error against the CFL numbers. The error for the transmission coefficient is same with the reflection. As the CFL number increases, the error becomes small. The reason of large error in small CFL number has responsible the numerical dispersion error. It is confirmed that the present formulation for density variation is valid.

References

1. K. S. Yee: IEEE Trans. Antennas Propag., **AP-14** (1966) 302.
2. K. Kowalczyk and M V. Walstijn: IEEE Trans.

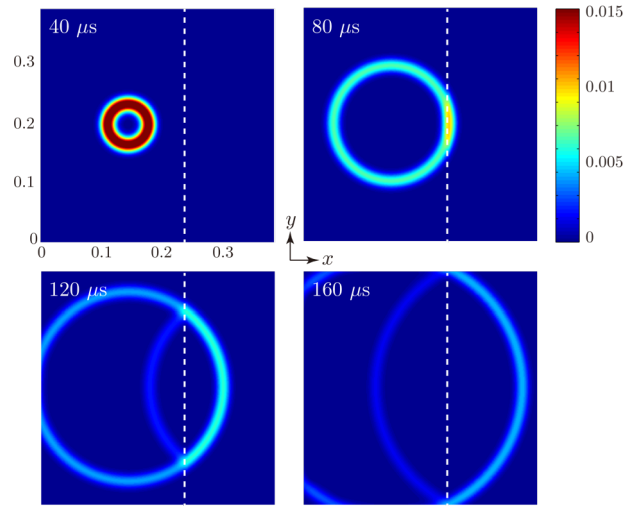


Fig. 4 Sound pressure distributions.

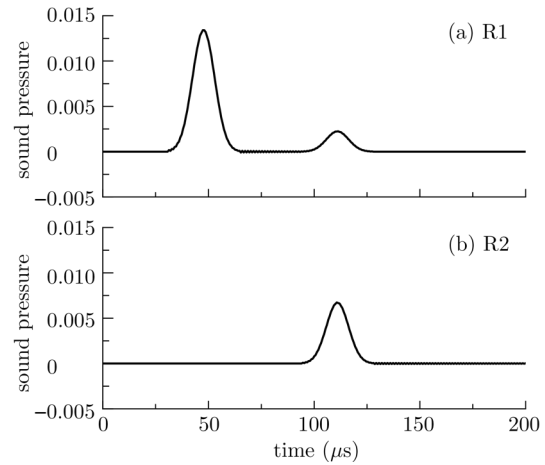


Fig. 5 Calculated waveforms at the receiving points R1 and R2.

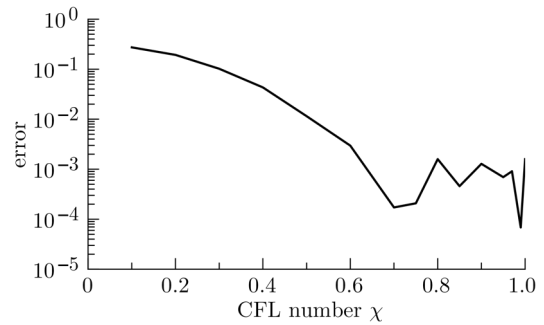


Fig. 6 Estimated error for the reflection coefficient against theoretical value.

- Audio Speech and Lang. Process., **19** (2011) 34.
3. T. Ishii, T. Tsuchiya, and K. Okubo: Jpn. J. Appl. Phys., **52** (2013) 07HC11.
4. O. Yamashita, T. Tsuchiya, Y. Iwaya, M. Otani, and Y. Inoguchi: Jpn. J. Appl. Phys., **54** (2015) 07HC02.